Multifractal properties of temperature fluctuations in turbulence

François G Schmitt, Daniel Schertzer, Shaun Lovejoy, Yves Brunet

MULTIFRACTAL PROPERTIES OF TEMPERATURE FLUCTUATIONS IN TURBULENCE

F. SCHMITT [a], D. SCHERTZER
Laboratoire de Météorologie Dynamique, Université Paris VI, 4, place Jussieu, 75005 Paris, France

S. LOVEJOY
Physics Department, McGill University, Montréal, PQ, H3A 2T8, Canada

Y. BRUNET
INRA Bioclimatologie, BP 81 33883 Villenave d'Ornon Cédex, France

We analyse the scaling properties of the temperature field in turbulence. We review different recent multifractal proposals for the structure functions' scale invariant exponents of the temperature field, linked to different types of infinitely divisible multiplicative models: log-normal, log-Lévy and log-Poisson multifractals. Using a temperature database, we test these models. We also consider the influence of the number of samples studied, on the maximum reachable singularity. We conclude with a discussion on the influence of the signs of the fluctuations.

1 Multifractal models for the temperature field

1.1 Phenomenological relations

The temperature field is usually studied in turbulence by considering the temperature shear at scale ℓ, $\Delta\theta_\ell = |\theta(x+\ell) - \theta(x)|$. Using dimensional analysis, Obukhov and Corrsin [1] obtained a well-known relation giving the temperature fluctuations in the inertial range with the help of two fluxes, which they assumed constant:

$$\Delta\theta_\ell \sim (\chi_\ell)^{1/2} (\epsilon_\ell)^{-1/6} \ell^{1/3} \tag{1}$$

where $\sim$ means proportionality and ϵ_ℓ and χ_ℓ are respectively the energy flux and scalar variance flux through scale ℓ. In order to take intermittency into account, these fluxes, which are conserved by the equations of motion [2], are often considered to cascade from large scales to small, via multiplicative cascades [3–5]. This leads to multifractal fields, whose statistics can be defined by their moments [5]:

[a] Now at Université Libre de Bruxelles, Section Chimie Physique, CP 231, Bld du Triomphe, B-1050 Bruxelles, schmitt@oma.be

$$< (\epsilon_\ell)^q > \sim \lambda^{K_\epsilon(q)} ; < (\chi_\ell)^q > \sim \lambda^{K_\chi(q)} \tag{2}$$

where L is a fixed outer scale and $\lambda = L/\ell$ is the corresponding scale ratio, q is the order of moment and $K_\epsilon(q)$ and $K_\chi(q)$ are the scale invariant moment functions for the fluxes. These scale-invariant functions describe all the statistics of the fluxes – at all scales and for all intensities. Due to the conservation – in ensemble average – of the fluxes, we consider their mean to be scale invariant: $K_\epsilon(1) = 0$ and $K_\chi(1) = 0$. These multifractals are often said to be conservative multifractal fields. On the other hand, Eq. 1 expresses that the temperature shears are obtained through a fractional integration ($\ell^{1/3}$ factor) of a non-linear product of the two fluxes. Let us denote the scaling properties of the temperature field as:

$$< (\Delta\theta_\ell)^q > \sim \ell^{\zeta_\theta(q)} \tag{3}$$

where $\zeta_\theta(q)$ is the structure functions' scale invariant exponent of the temperature field. In order to characterize the scaling statistics of temperature turbulence, one of the interesting points is to relate $\zeta_\theta(q)$ to $K_\epsilon(q)$ and $K_\chi(q)$, as is done in [6]; another approach involves the characterization of $\zeta_\theta(q)$ directly, using one of the different cascade models available, as done in [7,8]. We recall the different cascade models and compare the results in the following sections.

1.2 Infinitely divisible continuous cascade models for the temperature turbulent field

Several recent studies emphasized the necessity to consider infinitely divisible cascade models in turbulence [9–13], originally called "continuous cascades" [5]: this means that one can densify (in scales) the cascade between the larger scale and the smaller, reaching a continuous (in scale) cascade model. Using the "canonical representation" (also termed Lévy-Khinchine representation) for infinitely divisible random variables (see [14]), one obtains Lévy-stable [5,12] or (under weaker asumptions) Poisson [15,16,11] statistics.

Temperature parameters for strong universality. – In the former case, which we called in [12] "strong universality" because Lévy-stable variables are stable and attractive [14], one can represent $\zeta_\theta(q)$ in the following form [5,12]:

$$\zeta_\theta(q) = qH - \frac{C_{1\theta}}{\alpha - 1} (q^\alpha - q) \tag{4}$$

where H is the degree of non-conservation of the average of the field ($H = \zeta_\theta(1)$): when $H \neq 0$ the average is scale-dependent; the second term expresses

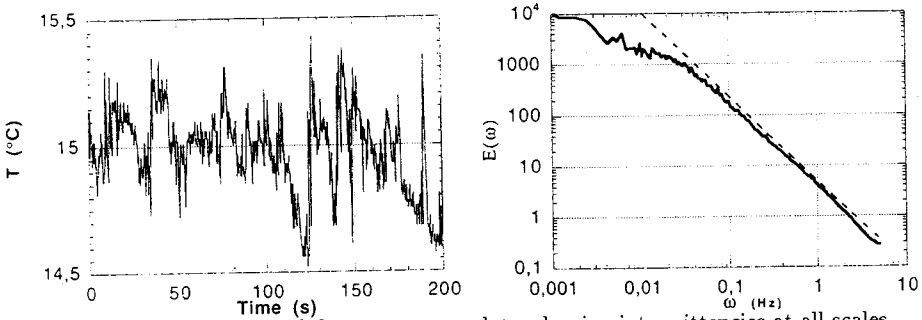

Figure 1: (Left) A sample of the temperature data, showing intermittencies at all scales.

Figure 2: (Right) The Fourier power spectrum of the data, in log-log plot, showing a power-law for about 2 decades, with a slope of $\beta \sim 1.62$: a dotted straight line of slope $-5/3 \sim -1.67$ is shown for comparison.

a deviation from homogeneity of the flux (for homogeneous fluxes, $\zeta_\theta(q) = qH$), and represents the intermittency corrections; $C_{1\theta}$ is the fractal codimension of the mean of the process ($0 \leq C_{1\theta} \leq d = 1$ for a $1D$ dataset), and α is the Lévy index (of the generator, which is the *log* of the multiplicative process): $0 \leq \alpha \leq 2$. We use here the results presented in [6] to propose some values for these parameters $H, C_{1\theta}, \alpha$. Assuming independence between temperature and velocity fluctuations, we proposed in [6] the following relation:

$$\zeta_\theta(q) = q/3 + K_\epsilon(q/6) - K_\chi(q/2) \tag{5}$$

where $K_\epsilon(q)$ and $K_\chi(q)$ are given by the following relation for conservative (strong) universal multifractals:

$$K(q) = \frac{C_1}{\alpha - 1}(q^\alpha - q) \tag{6}$$

We empirically obtained in [6] the following values (see below for a presentation of the databases): $\alpha_\epsilon \simeq 1.5 \pm 0.1$, $C_{1\epsilon} \simeq 0.16 \pm 0.02$ and $\alpha_\chi \simeq 1.4 \pm 0.1$, $C_{1\chi} \simeq 0.22 \pm 0.02$. We can link Eq. 5 to Eq. 4 taking for simplicity the value $\alpha_\epsilon \simeq \alpha_\chi \simeq 1.45 \pm 0.15$ ($\equiv \alpha$). Then Eqs. 6, 5 and 4 give:

$$H = \zeta_\theta(1) = 1/3 + K_\epsilon(1/6) - K_\chi(1/2) \tag{7}$$

$$C_{1\theta} = \frac{C_{1\chi}}{2^\alpha} - \frac{C_{1\epsilon}}{6^\alpha} \tag{8}$$

With the above values, this gives: $H \simeq 0.37 \pm 0.02$ and $C_{1\theta} \simeq 0.07 \pm 0.005$. We will test below the parametrisation given by Eq.4 and these values.

Temperature parameters for weak universality. – In the second case, which we called in [12] "weak universality" because Poisson laws are infinitely divisible but not stable nor attractive, the temperature structure functions' scaling exponent can be written [15,16,11]:

$$\zeta_\theta(q) = q(H - \gamma^+) + \left(1 - \left(1 - \frac{\gamma^+}{c}\right)^q\right) c \tag{9}$$

where H is still given by $H = \zeta_\theta(1)$, γ^+ is linked to a maximum singularity (see below for more precise presentation of singularities in this framework) $\gamma_{max} = \gamma^+ - H$, and c is the fractal codimension of this maximum singularity. Indeed, a hypothesis of this model is that $0 \leq 1 - \gamma^+/c \leq 1$, so that there is an asymptotic behaviour for $\zeta_\theta(q)$, when $q \to \infty$: $\zeta_\theta(q) = q(H - \gamma^+) + c$. As we showed in [12], this model is in fact a particular scale densification of the (Bernouilli process) α-model [17]. A different densification leads to the log-normal multifractal [9].

Recently, Ruiz *et al.*[8] empirically proposed the numerical values: $H - \gamma^+ \simeq 0.06 \pm 0.02$, $1 - \gamma^+/c \simeq 0.63$, $H \simeq 0.37$, which give $\gamma^+ \simeq 0.31$ and $c \simeq 0.84 \pm 0.1$[b]. We test this proposal below.

2 Empirical validation

2.1 *Power spectrum and empirical values of $\zeta_\theta(q)$ for $q \leq 5$*

We analyse here temperature data, recorded with a sonic anemometer in the atmosphere 25m above ground, over a pine forest in south-west France, with a sampling frequency of 10Hz. We analysed 22 profiles of duration 55 minutes each. A sample of the data is shown in Fig.1. The power spectrum is shown in Fig.2, in log-log plot. The straight line in this figure indicates a scaling behaviour following:

$$E_\theta(\omega) \sim \omega^{-\beta} \tag{10}$$

where $E_\theta(\omega)$ is the temperature Fourier power spectrum, and ω is the frequency. In the following, the mean wind velocity of 2.7 ms^{-1} allows us to transform temporal into spatial increments, using Taylor's hypothesis [18], assuming that the small-scale turbulent fluctuations are advected by the large-scale velocity. β is the exponent of the scaling of the power spectrum, which is related to the second order moment exponent of the structure function: $\beta = 1 + \zeta_\theta(2)$. Here we obtain $\beta \sim 1.62$, which is less steep than the $-5/3 \sim -1.67$ slope which would be obtained in case of homogeneous Obukhov-Corrsin turbulence [1] (see

[b] They indicated $c \simeq 0.80$, but 0.84 is more coherent with the other values they obtained.

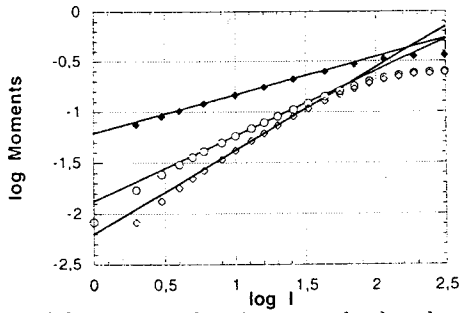

Figure 3: The scaling of the structure functions: on a log-log plot, the straight lines indicate the range of the scaling, and their slopes give estimates of $\zeta_\theta(q)$; from top to bottom: $q = 1, 2, 3$.

Eq. 1). This is in agreement with the value reported in [19], and shows that the "intermittency correction" to the famous "-5/3 law" for temperature is in opposite sign as for velocity. This also shows the range of scales for which the scaling is expected to occur.

We computed the structure functions according to Eq. 3. Figure 3 shows the scaling of the structure functions for various orders of moments: in log-log plot, the straight lines are estimates for $\zeta_\theta(q)$. We choose here for the linear interpolations the three first decades; the scaling may seem to be very good only for one and a half decade: we also used the so-called "Extended Self-Similarity" (ESS), as in [19, 8]: this gave nearly the same values for $\zeta_\theta(q)$.

In Fig. 4 we show the resulting function $\zeta_\theta(q)$, for moments up to order 5 (with a 0.1 increment). For comparison, we also plotted in the same figure the results reported in [20] and in [19]. The theoretical fits given by Eqs.9 and 4, for respectively the log-Poisson and "log-Lévy"[c] models, with the values proposed in Section 1.2, are shown in the same figure. The very good correspondence observed in this figure indicates that these two models are compatible with the data up to relatively medium order of moments ($q \leq 5$).

2.2 *Non-analycity of* $\zeta_\theta(q)$

A striking consequence of universal multifractals is that $K(q)$, $\zeta(q)$, and other related quantities such as $f(q) = q\zeta'(0) - \zeta(q)$ (when $\alpha > 1$) are non-analytic at $q = 0$. Using Eq.4, we see that $f(q)$ is precisely a non-integer power law proportional to q^α. Therefore, on a log-log plot, $f(q)$ vs. q should display a slope of α. In Fig. 4, two straight lines are also represented. One corresponds to the

[c]The term "log-Lévy" is not so correct, because the observables correspond to an integration of the pure log-Lévy field, leading to multifractal phase transitions.

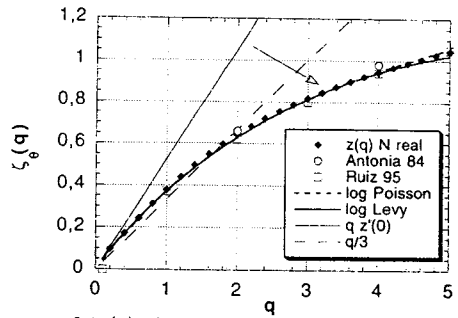

Figure 4: Our estimates of $\zeta_\theta(q)$ plotted vs. q, for moments up to order 5. Also shown for comparison the values reported in other studies: all the empirical data we report here are very close to each other. The thin continuous lines correspond to the theoretical models proposed in the text: this shows that the fits are very good, and that each of these two models can be considered to be compatible with the data for $q \leq 5$.

homogeneous Obukhov-Corrsin case: $\zeta_\theta(q) = q/3$, and the second corresponds to the tangency in 0, according to Eq. 4: $\zeta_\theta(q) = q\zeta'_\theta(0)$, with:

$$\zeta'_\theta(0) = H + \frac{C_{1\theta}}{\alpha - 1} \quad ; \alpha > 1 \tag{11}$$

The values we gave for H, $C_{1\theta}$ and α yield $\zeta'_\theta(0) \simeq 0.53$. We represented in Fig. 5 $f(q)$ vs. q in a log-log plot. If Eq. 4 is correct, this should give a straight line with a slope of $\alpha < 2$; in case of analycity, the slope should be 2. Figure 5 represents also, with a straight line, the model obtained from Eq. 4 and with a dotted line the model given by Eq. 9: the straight line of slope $\alpha = 1.45$ fits very well the data, confirming the non-analycity. We see on this Figure that for very low order of moments there is a deviation from the straight line: this comes from a limitation of the measuring sensor, wich prevents us from exploring low order singularities, i.e. low orders of moments. The log-Poisson model represented by the dotted line seems to be relatively good fitting: this comes from the fact that we cannot explore sufficiently low orders of moment. The other important aspect of the log-Poisson model is an hypothesis of a fixed larger singularity, a question we consider below.

2.3 *Influence of the number of samples*

In the multifractal framework, every order of moments is associated with an order of singularity, which depends on the scales in the following way:

$$\Delta\theta_\ell \sim \Delta\theta_L \left(\frac{L}{\ell}\right)^\gamma \tag{12}$$

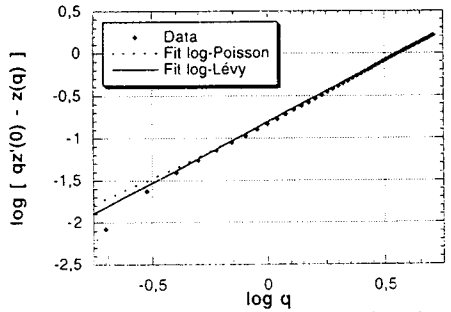

Figure 5: The non-analycity tested on the data, compared to the two models studied here, in log-log (decimal log) plots. A straight line of slope smaller than 2 (giving here $\alpha \simeq 1.45$) is an indication of non-analycity, and thus a confirmation of the validity of the log-Lévy model.

where γ are the orders of singularity, which are usually negative. For homogeneous turbulence, there is only one singularity $\gamma = -1/3$; for monofractal models there are many orders of singularity (up to $C_1 - H$), but they all have the same (unique) fractal codimension. For multifractal models, there is a whole range of singularities, associated with the moments via a Legendre transform [21]:

$$c_\theta(\gamma) = \zeta_\theta(q) + q\gamma \quad (13)$$

$$\gamma = -\zeta_\theta'(q) \quad (14)$$

where $c_\theta(\gamma)$ is the codimension of the singularity γ, defined using the probability distribution [5]:

$$Pr\left(\Delta\theta_\ell \geq \Delta\theta_L \left(\frac{L}{\ell}\right)^\gamma\right) \sim \left(\frac{\ell}{L}\right)^{c(\gamma)} \quad (15)$$

Equation 14 expresses the fact that for multifractal processes, $\zeta_\theta(q)$ is nonlinear. Furthermore, it shows that when there is a maximum singularity γ_{max}, $\zeta_\theta(q)$ becomes linear for $q \geq q_{max}$, where:

$$q_{max} = c_\theta'(\gamma_{max}) \quad (16)$$

$$\zeta_\theta(q) = c_\theta(\gamma_{max}) - q\gamma_{max} \quad q \geq q_{max} \quad (17)$$

The nature of asymptotic behaviour of $\zeta_\theta(q)$ is an important question in turbulence (for velocity as well as for passive scalar turbulence).

Although, the general "canonical" multifractals have no upper bound on their orders of singularity (this is true for example of the universal multifractals

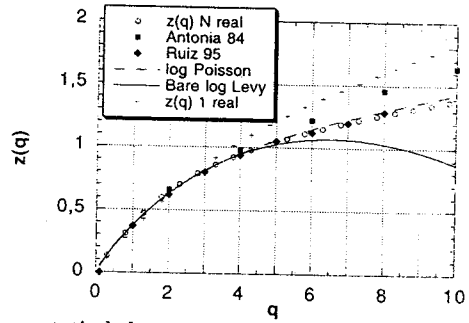

Figure 6: The asymptotic behaviour of the scale invariant moment function for the temperature field, for 1 and 704 samples, compared to the two models studied here. We may note that the empirical departure from the "bare" log-Lévy model is expected, because observables are associated to multifractal phase transitions. This arises here at the moment of order 5.

with $\alpha \leq 1$), multifractal processes do exist with intrinisic upper bounds. For example the α model, p model, log-Poisson model and universal multifractal model with $\alpha < 1$ all have bounded γ. However even when an intrinsic bound exists, it may not be observable in a finite sample, simply because the latter is too small implying that the corresponding probability is too low. This effect of finite sample size leads to multifractal phase transitions [23, 22], which can be either of first or second order. The particularly interesting first order case is a consequence of a finite dimensional integration of the process for example by the measuring device (see below).

For the log-Poisson model, as we already saw, there is an upper bound on the singularities, even in case of infinite sample size. This is a basic hypothesis of the model. On the other hand, for the log-Lévy model, there is no theoretical upper bound for the singularities, and the empirical estimates have a limit only because of the finite size of the sampling. We study below the empirical estimates of $\zeta_\theta(q)$ for 1 and ~ 700 realizations, and the influence of the number of realizations on the asymptotic behaviour, as we did in [12, 23] for turbulent velocity.

To study the influence of the number of samples, we decomposed our data series into 704 different portions of length 512 datapoints each (the maximum scale ratio for the scaling range is about 500). First, we considered the estimate of $\zeta(q)$ (we drop the subscript θ for simplicity) for one sample. For each segment i of the dataset, we estimate $\zeta^i(q)$. We then take the mean of all these

exponents $\zeta^i(q)$ as being $\zeta_1(q)$, the scale invariant function for one segment:

$$\zeta_1(q) = \frac{1}{704} \sum_{i=1,704} \zeta^i(q) \tag{18}$$

This is shown in Fig. 6. The linear asymptote has the equation $\zeta_1(q) = 0.11q + 0.68$, for $q \geq 4$.

When more (than one) sample is taken into account for moment estimates, the slope of this straight line decreases, and the intercept increases. For 704 samples, we evaluate $\zeta_{704}(q)$ using an ensemble average for all the samples in Eq. 3[d]. This is also shown in Fig. 6. The linear asymptote has here the equation $\zeta_{704}(q) = 0.06q + 0.78$, for $q \geq 5$. One may note that this is not far from the asymptote proposed in [8], which was empirically $0.06q + 0.84$. But this does not confirm this model: these values were fitted in [8] using their empirical asymptote, which for a single sample happens to be roughly the same as ours; but the log-Poisson model implies that this asymptote is already reached for one sample, whereas we just saw that this is not the case. This change of the slope and intercept of the asymptote with the number of samples is therefore a clear argument against the log-Poisson model.

2.4 The question of signs and complex cascades

We discuss here briefly the question of the signs of the fluctuations. In Eq. 12, the fluctuations are obtained from the singularities (the "generator" of the field) throught an exponentiation. This means that for real singularities, one describes only the positive fluctuations, *i.e.* their amplitude. To take into account the signs of the fluctuations, one possibility is to consider the real part of a complex cascades (see [24] for a first presentation, and [25] for a wider generalization involving Lie cascades).

In this framework, we may assume the moments to be written:

$$< (\Delta\theta_\ell)^q > \sim \left(\frac{\ell}{L}\right)^{\zeta(q)+iZ_I(q)} \tag{19}$$

where $Z(q) = \zeta(q) + iZ_I(q)$ ($i^2 = -1$) is the complex scale invariant structure function exponent. Taking the real part of this relation, we obtain a correction to the "pure" scaling, involving a cosine:

$$\frac{Re\,(< (\Delta\theta_\ell)^q >)}{(\ell/L)^{\zeta(q)}} \sim \cos\left(Z_I(q) \log\left(\frac{\ell}{L}\right)\right) \tag{20}$$

[d] Let us underline the distinction: $\zeta_{704}(q)$ is obtained through a log-log plot of the ensemble average of all the values of the moments, whereas $\zeta_1(q)$ is the mean of all the values obtained throught a log-log plot of the moments for each segment.

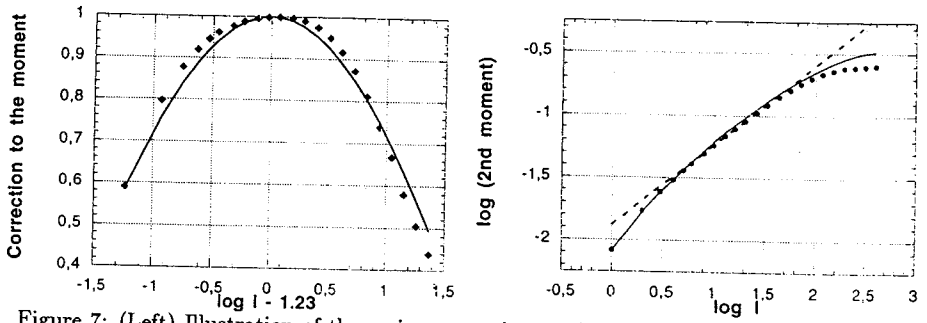

Figure 7: (Left) Illustration of the cosine correction to pure scaling, obtained in a complex framework, useful to take into account the signs of the fluctuations; dots: empirical values corresponding to the left-hand side of Eq.20., and continuous line: the right-hand side of Eq.20 with $Z_I(2) = 0.77$.

Figure 8: (Right) The moment of order 2, compared to the pure scaling (dotted straight line), and the scaling with signs correction (continuous line). This latter fit is quite close to empirical data; it could be an explanation of the slight concavity usually observed when studying the scaling of the structure functions.

This is shown in Fig. 7 for the moment order 2. A fit with $Z_I(2) = 0.77$ is shown, compared to the empirical estimates. In Fig. 8 the resulting correction for the scaling itself is shown: the data are compared to the straight line which would be obtained in case of a pure scaling, and also to a continuous line taking into account the sign corrections. We see that even if this continuous line doesn't exactly fit the data, it is quite close to the data, and could well explain the slightly concave behaviour usually obtained for the scaling of the structure functions.

We leave for the future studies of a more general estimate of $Z_I(q)$ for other orders of moments. This first step shows that it is certainly possible to describe the singularities in a complex framework, a task which would be useful to characterize the signs of the turbulent fluctuations. We also note that this approach may be an alternative explanation of ESS behaviour to that which is proposed in [8]: indeed if $Z_I(q)$ is proportional to $\zeta(q)$ the ESS effect is straightforward.

3 Conclusion

We have considered the scaling properties of the turbulent temperature field in a multifractal framework. We have compared two models (the log-Poisson model and the "strong" universal multifractals obtained from a log-Lévy field)

to empirical data, and given our point of view concerning the respective degree of empirical relevance of these models. We first showed that both models empirically fit well, and in a similar manner, the the moderate range of singularities and orders of moments. However, their extreme behaviours are quite different, and allow us to discriminate them. Althought more convincing arguments will require more precise measurements, we nevertheless showed that the scale invariant exponent of the temperature structure functions $\zeta_\theta(q)$ is non-analytical at the origin, as assumed for the log-Lévy model. On the other hand, we showed that the asymptote of $\zeta_\theta(q)$ depends on the number of samples, which is contrary to the basic log-Poisson hypothesis of a fixed maximum order of singularity (corresponding to the most extreme events). We also proposed a first step in the analysis of the influence of the signs of the fluctuations on this scale invariant exponent.

This work confirms the theoretical prediction that turbulence is a universal multifractal process and provides a phenomenological parametrisation which helps to describe nearly all the statistics of the amplitude of the temperature fluctuations in fully developed turbulence.

Acknowledgments

We thank Y. Chigirinskaya, D. Marsan and C. Naud for discussions, and S. Ciliberto for sending his preprints prior to publication.

References

1. A. Obukhov, *Izv. Akad. Nauk SSSR Geogr. I Jeofiz.* **13**, 55 (1949); S. Corrsin, *J. Appl. Phys.* **22**, 469 (1951).
2. A. S. Monin and A. M. Yaglom, *Statistical Fluid Mechanics: Mechanics of Turbulence*, Vol.II (MIT Press, Cambridge, 1975).
3. A. N. Kolmogorov, *J. Fluid Mech.* **13**, 82 (1962); A. Obukhov, *J. Fluid Mech.* **13**, 77 (1962).
4. A. M. Yaglom, *Sov. Phys. Dokl.* **2**, 26 (1966).
5. D. Schertzer and S. Lovejoy, *J. Geophys. Res.* **92**, 9693 (1987).
6. F. Schmitt, D. Schertzer, S. Lovejoy, and Y. Brunet, *Europhys. Lett.* **34**, 195 (1996).
7. F. Schmitt, D. Lavallée, S. Lovejoy, D. Schertzer and C. Hooge, *C. R. Acad. Sci. Paris, Série II* **314**, 749 (1992); Y. Chigirinskaya, D. Schertzer, S. Lovejoy and A. Ordanovich, *Nonlin. Proc. Geophys.* **1**, 105 (1994).
8. G. Ruiz-Chavarria, C. Baudet and S. Ciliberto, *Physica* D (in press).

9. D. Schertzer, S. Lovejoy, D. Lavallée and F. Schmitt, in *Nonlinear Dynamics of Structures*, ed. R. Sagdeev *et al.* (World Scientific, Singapore, 1991).
10. E. A. Novikov, *Phys. Rev.* E **50**, R3303 (1994).
11. Z. S. She and E. Waymire, *Phys. Rev. Lett.* **74**, 262 (1995).
12. D. Schertzer, S. Lovejoy and F. Schmitt, in *Small Scale Structures in 3D Hydro and MHD Turbulence*, ed. M. Meneguzzi *et al.* (Springer-Verlag, 1995).
13. B. Castaing, *J. Phys. II France* **6**, 105 (1996).
14. W. Feller, *An Introduction to Probability Theory and its Applications*, Vol.II (Wiley, New York, 1971).
15. Z. S. She and E. Levêque, *Phys. Rev. Lett.* **72**, 336 (1994).
16. B. Dubrulle, *Phys. Rev. Lett.* **73**, 959 (1994).
17. D. Schertzer and S. Lovejoy, in *Turbulence and chaotic phenomena in fluids*, ed. T. Tatsumi (North-Holland, 1984).
18. G. I. Taylor, *Proc. Roy. Soc.* A **164**, 476 (1938).
19. G. Ruiz-Chavarria, C. Baudet and S. Ciliberto, *Europhys. Lett.* **32**, 413 (1995).
20. R. A. Antonia, E. J. Hopfinger, Y. Gagne and F. Anselmet, *Phys. Rev.* A **30**, 2704 (1984).
21. G. Parisi and U. Frisch, in *Turbulence and Predictability in Geophysical Fluid Dynamics and Climate Dynamics* ed. M. Ghil *et al.* (North-Holland, 1985).
22. D. Schertzer and S. Lovejoy, *J. Appl. Meteo.* , in press (1997).
23. F. Schmitt, D. Schertzer, S. Lovejoy and Y. Brunet, *Nonlin. Proc. Geophys.* **1**, 95 (1994).
24. G. Brethenoux, D. Mitrani, J. Dezani, D. Schertzer and S. Lovejoy, *EOS* Suppl. **73**, 57 (1992).
25. D. Schertzer and S. Lovejoy, in *Space/time Variability and Interdependence for Various Hydrological Processes* ed. R. Feddes (Cambridge University Press, 1995).